Towards a silicon monolithic suspension

Flavio Travasso[1,3], Helios Vocca[2,3], Antonfranco Piluso[2,3], Damiano Aisa[2,3], Takayuki Tomaru[4], Takafumi Ushiba[5], Toshikazu Suzuki[5], Takaharu Shishido[4], Ursula Gibson[6], John Ballato[7], Thomas Hawkins[7],

[1] School of Sciences and Technology, University of Camerino, I-62032 Camerino, Italy
[2] Department of Physics and Geology, University of Perugia, I-06123 Perugia, Italy
[3] INFN Perugia, I-06100 Perugia, Italy
[4] National Astronomical Observatory of Japan, 2-21-1 Osawa, Mitaka, Tokyo 181-8588, Japan
[5] Institute for Cosmic Ray Research, 5-1-5 Kashiwanoha, Kashiwa, Chiba 277-8582, Japan
[6] Norwegian University of Science and Technology, IFY, Høgskoleringen 5, 7491 Trondheim, Norway
[7] Department of Materials Science and Engineering, Clemson University, Clemson, SC 29634, USA

May 12, 2020

Abstract

The thermal noise of the main optics is a fundamental limit to the sensitivity of present and future gravitational waves interferometers. To reduce it, the next generation of interferometers will adopt larger mirrors and cryogenic solutions. To reach this goal, it is important to identify suitable materials for substrates and suspensions. That means not only materials with good thermal, mechanical and optical properties, but also materials that allow extended substrates and thin, long and strong fibers. Sapphire is a good candidate and it is already used in the KAGRA experiment, but it is hard to work and polish and is very expensive. Moreover, the production of substrates larger than 20 cm in diameter presents many difficulties. A very promising alternative candidate is silicon. With present work, we report the status of the R&D project on silicon monolithic suspension, the results obtained so far on fibers produced with three methods and the strategies to improve them. We also present a protocol to characterize silicon bulks under cryogenic conditions before installation and the control system to reduce the seismic noise on the suspended substrates.

DOI: 10.5281/zenodo.3820523

Introduction

The next generation of GW interferometers will be larger, with new geometries, some of them will be built underground, but for sure all of them will operate under cryogenic condition [1, 2]; hence the search for materials with very stringent mechanical and optical properties at low temperature. For the last suspensions stage of the main interferomenter optics, this means looking for materials with:

- good thermal conductivity (suspensions, substrates)
- high breaking strength (suspensions)
- low thermal noise (suspensions, substrates)

- low optical absoption and birefringence (substrates)

Such materials should also allow the production, machining and polishing of substrates with a diameter of about 0.5m and thin fibers with diameter of about 1mm and length of about 1m. Sapphire is a good candidate, being already used by KAGRA [3], but it is very expensive and so fragile that production, machining and polishing processes present many difficulties. A very promising alternative candidate is silicon: it is *abundant, inexpensive, and can be produced and processed controllably to unparalleled standards of purity and perfection*[6]. Moreover, silicon shows a thermal conductivity between 10K and 20K (operating temperature of KAGRA and future GW detectors [1][3]) very similar to that of sapphire (Fig.7). Its maximum breaking strenght is half that of the sapphire [4] but latter point deserve a clarification. Fibers breaking strength strongly depend on many parameters such as the quality of the surface [6]. Chemical etching does not affect sapphire while it is a well known and developed technique for silicon [5] and allows to significantly improve the surface quality of silicon fibers (Fig.6) and consequently its breaking strength. Furthermore, current production is already capable of producing large substrates of extremely pure silicon.

Monolithic suspension design

To design monolithic suspensions, the mechanical constrains of the whole payload[1] would reconsidered to reduce the suspension thermal noise and increase their reliability. In the next generation of GW detectors, more than 100 kg heavy mirrors will be suspended at cryogenic temperatures. The suspensions will be designed not only to withstand these loads (3 times the load of the current mirrors), but also to eliminate the heat released by the laser on the mirror, have low thermal noise, and allow precise control [7]. In this perspective, it is important to first characterize fibers and substrates from a thermal and mechanical point of view and then define their final design. The next step will be to check the thermal noise of the entire payload to evaluate the contribution and interaction of each element and then optimize them.

[1]From reference [7] - "In AdV, the input and end mirrors are all suspended from a steel marionette which, in turn, is suspended to the last filter of the superattenuator. The marionette and the mirror form a double-pendulum system, surrounded by a rigid structure called cage. The assembly of the marionette-mirror pendulum system with the cage and associated auxiliary optics and actuators is referred to as the payload. The payload is conceived for the compensation of residual seismic motion and for acting on the test masses working point in the interferometer. Whereas a full description is available in the paper [8].

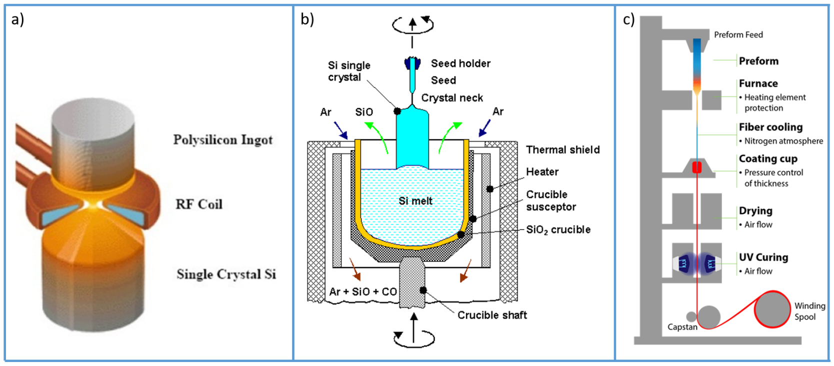

Figure 1: Production methods: a) Scheme of the Float Zone growth method; b) Scheme of the Czochralski growth method; c) Scheme of a drawing tower for the production of optical fibers.

Fibers production and tests

In the next generation of GW detectors, the adopted solution for the suspension design will be a compromise between mechanical, thermal and control issues. The first important step to consider is the production method: silicon samples produced with three different methodologies are analyzed (Fig.1).

- *Grinded-etched silicon fibers - Czochralski growth method*[2]

  Five undoped silicon bars, 1cm in diameter and 15 cm long, produced with the Czochralski growth method [10], are mechanically machined to reduce their diameter down to 1 mm. The quality of their surface, was improved by mechanical polishing; finally, a 100-200 μm thick outer layer is removed by a chemical treatment. The orientation of the fibers is [100] along their axis;

- *Grinded-etched silicon fibers - Float Zone growth method*[2]

  Three undoped and two (p-type and n-type) doped silicon bars, produced with the Float Zone growth method [11], are mechanically machined so as to reduce their diameter down to 1 mm. Then mechanical and chemical polishing is perfomed as above to improve the quality of their surfaces. The orientation of their crystal axis is [111] along the fibers;

- *Silicon-core/Silica-clad optical fibers*[3]

  Refences [18, 19] well detail the production of optical fibers where a silicon core of about 0.15mm in diameter is surrounded by a silica cladding about 1.5mm thick. Once produced, the silicon core is polycrystalline, but a special annealing process results in a single crystalline core. A hydrofluoric acid bath removes the silica cladding without affecting the core. So far, four fibers were produced: one undoped silicon fiber oriented [111] along the fiber axis, one germanium doped silicon (Ge 6%) fiber with orientation [100] and two polycristalline silicon fibers.

[2]Impex HighTech GmbH — Mendelstraße 11, 48149 Münster.
[3]Clemson University, Norwegian University.

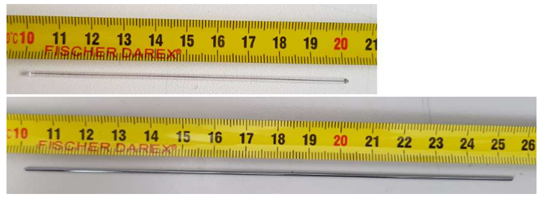

Figure 2: Silicon fibers: UP - Slicon-core/silica-clad fiber; DOWN - grinded-etching silicon fiber.

The reason for choosing fibers produced with different techniques, orientation of the crystals, dopants and surface quality, is based on the different mechanical and thermal properties (Young's modulus, Poisson ratio and so on) that silicon shows when these characteristics vary [4][5][6]. To measure loss angle, thermal conductivity, breaking strength, chemical and structural composition of surfaces and bulk, a series of tests were perfomed such as EDX-SEM, Raman, XRD and mechanical losses measurement [9]. At the moment it was possible to study only some of them (e.g. thermal conducitivy, Fig.7). Any trend will be clearly shown only after a complete study.

Grinded-etched fibers

Due to the similarity of their geometry, all the grinded-etching fibers were measured using the same setup and instrumentations.

Loss angle measurement - To measure the loss angle[4], one side of the fiber was strongly clamped to a massive support between two pieces of aluminum. No load is added to reduce the recoil losses. Fiber normal modes are excited through an electrostatic exciter driven by a high voltage amplifier and function generator. The decay time is acquired through a shadow sensor (Fig.3)[15].

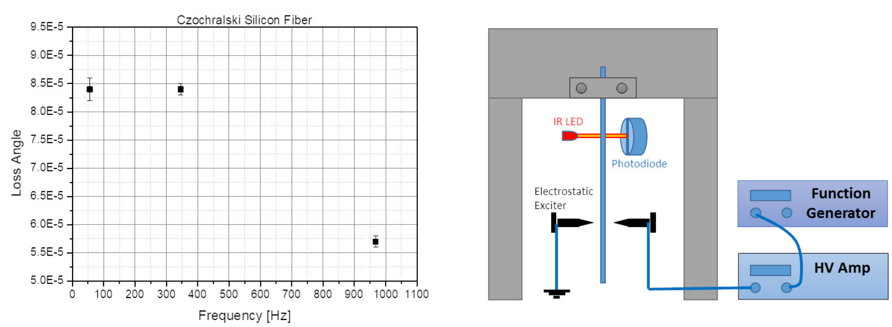

Figure 3: Loss angle measurement of grinded-etched silicon fibers: LEFT-loss angle measurement; RIGHT-loss angle measurement setup.

Figure 3 indicate a rather high loss angle compared to the values expected from the literature (($\phi_{th} \sim 10^{-7} - 10^{-8}$) [17]. Such behavior is likely to be explained with the losses due to the clamping system, the surface roughness (Fig.6) or the presence of internal defects.

[4]Dissipation measurements are an indirect way to evaluate thermal noise on a complex system and on its individual components [9]. This method is based on the measurement of the mechanical quality factor Q of the fibers. The inverse of the measured Q (the so-called loss angle ϕ) is proportional to the mechanical losses of whole system ($\phi_{meas} = \phi_{fiber} + \phi_{clamp} + \phi_{extra}$). Then using the fluctuation-dissipation theorem [12, 13] and the Levin method [14], it is possible to evaluate the fiber thermal noise [9, 16].

Clamping losses - To reduce the clamping losses, different options are possible. The first one foresees the use of steel clamps with polished surfaces and precision pins to avoid losses due to the elasticity/softness of aluminum used so far and to reduce losses due to any mechanical asymmetry [20]. Another promising solution is the use of a nodal system optimized for fibers [21][24]. A more attractive option is the production of fibers with large heads (Fig.4). This last solution would not only reduce the clamping losses, but it also come closer to the fiber final design [7].This strategy is the most difficult, but also the most interesting. All the groups involved in the project are currently working in this direction.

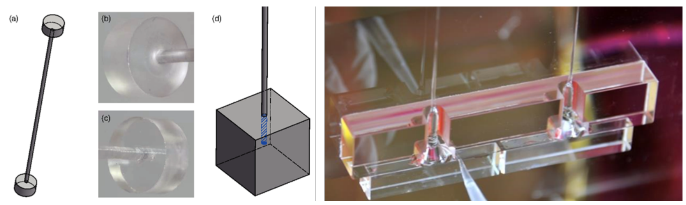

Figure 4: Fibers with heads: LEFT - KAGRA sapphire fibers; RIGHT - VIRGO silica fibers.

Surface and bulk defects - From the literature [4][5], the tensile strength of silicon is 7GPa while we obtained a much smaller value of about 90MPa. Possible reasons for such a big discrepancy could be the presence of bulk defects (point defects, dislocations, grains and so on) or surface defects (micro-crack)[5]. Concerning bulk defects, the fiber rupture surfaces, after the breaking test, were analyzed with an EDX-SEM. Figure 5 shows a bulk defect as a possible starting point of the rupture. This indicates the need to improve the quality of silicon rods production.

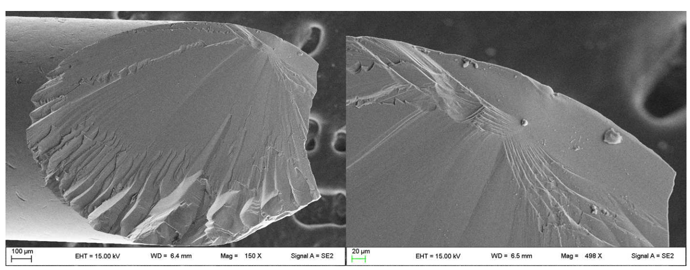

Figure 5: SEM pictures of a broken surface after the breaking strength test with two different magnifications: it is possible to see where the breaking started.

Figure 6 shows the surfaces of fibers: the grinded-etched fibers have a relative poor surface quality. To overcome this problem, better and deeper chemical etching and heat treatments with a pulsed laser are going to be tested in the next months. Moreover, we are investigating the chance to use the Float Zone method to melt/anneal thin fibers. This would improve both the surface and bulk quality. However, once the surface losses have been reduced and the clamping system has been optimized, it will be possible to verify the dependence of the loss angle on the production technique and on the dopants used.

[5]Breaking strength strongly depends on both surface and internal defects.

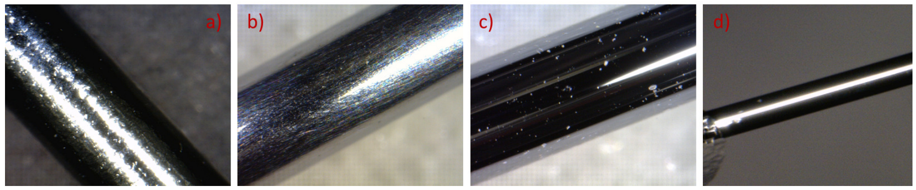

Figure 6: Silicon fibers surface: a) Grinded and ecthed fiber without a specific request on the surface roughness; b) Grinded and deeply ecthed fiber with SD 80-60; c) Grinded and deeply ecthed fiber with SD 60-40; d) Silicon core of the optical fiber.

Thermal coductivity - The fibers thermal conductivity was measured by KAGRA Cryo Group in their facilities in Japan[6]. Figure 7 compares the results with the expected data. Silicon fibers show a rather good agreement with the expected data even if the trend would seem to depend on the production method, probably due to the fact that silicon produced with Float Zone has less impurities and defects than CZ fibers [4]. The next step will be to test the effect of the dopants on the thermal conductivity.

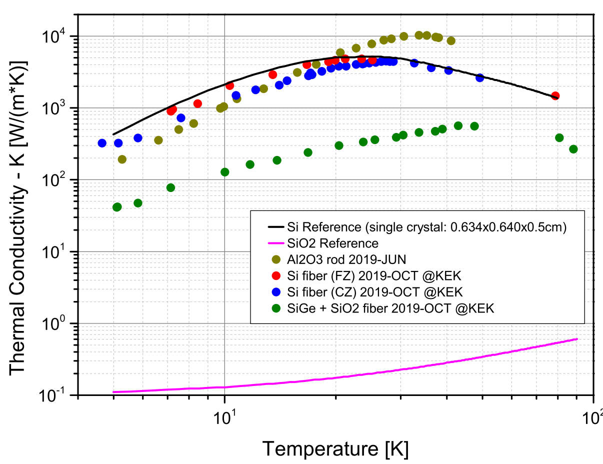

Figure 7: Thermal conductivity measurements of grown silicon and drawn silica-clad silicon-germanium core fibers. The results are compared with expected values for pure silicon and amorphous fused silica and with measured values of sapphire rods used in KAGRA.

Silicon/Silica fibers

Silicon-core/silica-cladding fibers look very promising: the production method (the drawing tower is shown in Fig.1) avoids any mechanical processing, thereby increasing the surface quality (Fig.6). Moreover, the use of thermal annealing to produce a monocrystalline fiber in a safe environment (the silica cladding) further improves the quality of the silicon core. The chemical etching, used to remove the cladding, not only does not affect the fiber core, but also removes any oxidized parts. Furthermore, the use of dopants inside the silicon facilitates the formation of a monocrystalline fiber

[6]KEK - High Energy Accelerator Research Organization, Tsukuba, Japan; ICRR - Institute for Cosmic Ray Research, Kashiwa, Japan.

[19]: the possible effects of dopants on mechanical and thermal properties are under study. Finally, the possibility of leaving the thicker parts of the preform on both sides of the fiber, to serve as the seed for heads (Fig.1, [18, 19]), is under test.

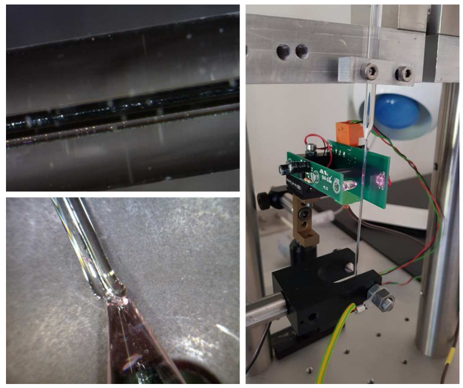

Figure 8: Loss angle measurement setup: LEFT-UP - silicon core surrounded by the silica cladding; LEFT-DOWN - Fiber welded to a silica rod; RIGHT - Measurement setup.

Loss angle measurement - The measurement setup is the same as for the grinded-etching fibers. First, the measurement of the loss angle of the entire silicon-core/silica-clad fiber is performed. Due to the silica cladding, the complete fiber is welded to a thicker silica rod to reduce clamping losses (Fig.8). Figure 9 shows the measured loss angle of the germanium (6%) doped silicon fiber. Although the values have improved compared to those of Figure 3, they are still far from the expected result of $\phi_{th} \sim 10^{-7} - 10^{-8}$. Plausible explanations would be the additional losses due to the friction between the core and the cladding or the effect of the germanium dopant. To verify the first option, we are currently removing the silica cladding and designing steel clamps optimized for such thin fibers. As for the second option, we can first measure the loss angle of the silicon-silica fiber with the pure silicon core, then remove the cladding and measure it again and finally compare all the results to evaluate the doping rule.

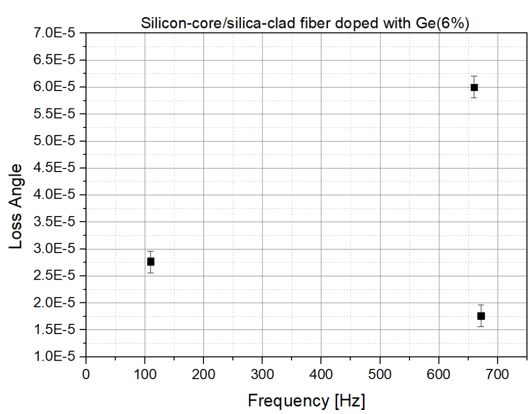

Figure 9: Loss angle measurements of the germaniume (6%) doped silicon fiber.

Surface and bulk defects - Figures 6 and 10 detail the surface quality of the fiber once the silica cladding is removed. The quality is really high and there are no noticeable defects. The only imperfections are due to external contaminants such as dust, some silica residues from the cladding and scratches due to the clamps used to handle the fiber. The EDX analysis was performed on the surface showing the absence of contaminants or oxidations.

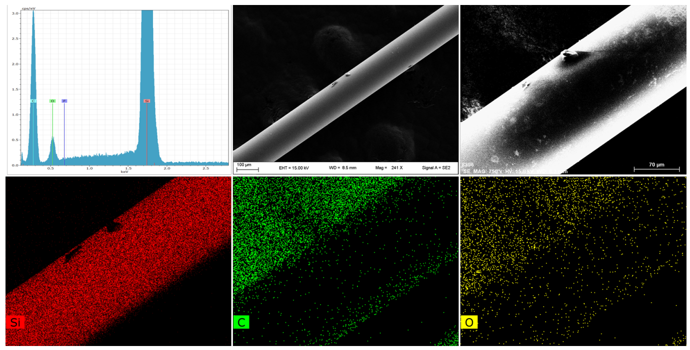

Figure 10: SEM analysis of the undoped silicon fiber once the silica cladding was removed: two particles of dust are well visible on the surface.

Useful information comes from the measurement of the mono-crystallinity of the fibers. This will be of fundamental importance when the payload will be assembled, since any cristalline defect (e.g point defects, dislocations, grains and so on) would decrease the breaking strength of the fibers. A measurement method was defined: by placing the thin fiber in the x-ray diffractometer, it is possible to find its maximum reflectivity (fiber crystal plane). Moving the fiber across the center of the diffractometer beam allows to x-scan its full length. Any cristalline defect would cause a change in the reflectivity or its total disappearance. A preliminary test was successfully carried out on the undoped fiber by partially removing the silica cladding (Fig.11). The X-ray results show good crystallinity in the analyzed region [18].

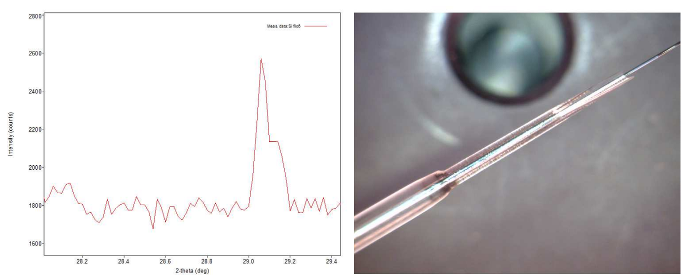

Figure 11: LEFT - X-ray diffraction of the undoped silicon fiber; HF etching on the undoped silicon fiber.

Thermal conductivity -

The silicon-silica fibers show appreciable differences with the expected values of the silicon and silica, as well. Its trend is a compromise between the two materials and seems to scale as the ratio of core diameters to cladding. This result could allow new strategies for the final design of the fibers in which the silica cladding can be removed only in specific regions to reduce thermal noise and left in others to allow the heads to be joined with the fibers

The next step for this type of fiber will be the total removal of the silica cladding to repeat all the mechanical and thermal measurements, leaving the break resistance measurement as the last test

Substrate test

To evaluate the thermal noise of a complex system such as monolithic suspensions, we have to measure the losses of each component and then estimate, through a FEM analysis [7], the contribution of each single element to the total thermal noise of the assembled payload [14]. In this way it is possible to optimize every single element. In this perspective, the proposed protocol forsees to measure the losses of the bare substrate, then the substrate with the bonded magnets[7], the substrate with the bonded magnets and the bonded lateral support and finally in the assembled suspensions. To measure the losses of the substrate at cryogenic temperature, a nodal system with low clamping losses [22, 23], was developed in collaboration with KAGRA Cryo Group.

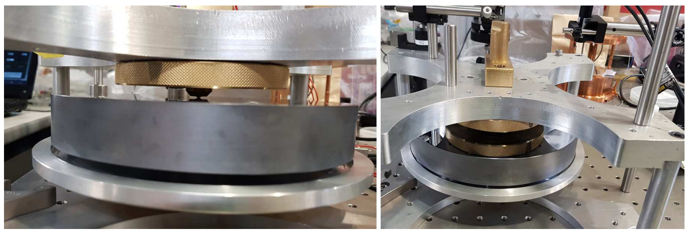

Figure 12: Nodal system developed in collaboration with KAGRA Cryo Group at ICRR.

Loss angle measurement -

In the nodal system, the substrate is positioned horizontally on a hemispherical support to reduce the contact surface. A second support with a load is placed on top of the substrate to increase stability (Fig. 12). To reduce the risk of scratching the substrate, the supports were suitably sized to find the right balance between the need to reduce contact losses and that of reducing the pressure at the point of contact.

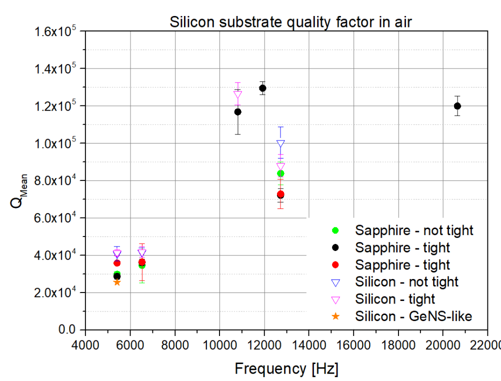

Figure 13: Q measurements in air of the silicon substrate using the nodal system in different configurations.

To get an indication on the best configuration of the supports, the system was tested in air with a silicon substrate 20cm in diameter, 3cm thick and weighing 2.2kg. Figure 13 reports the measured quality factor of the silicon substrate varying some parameters such as the use of one or two supports

[7]It is important not only to evaluate the contribution of the magnets to the total thermal noise, but also the contribution of the bonding. The same applies to each bonded item [7, 25].

or the force of tightening. The higher results were obtained using a lower support of silicon (radius of curvature of 12cm) and upper support of sapphire (radius of curvature of 0.3cm) only resting on the top of the substrate.

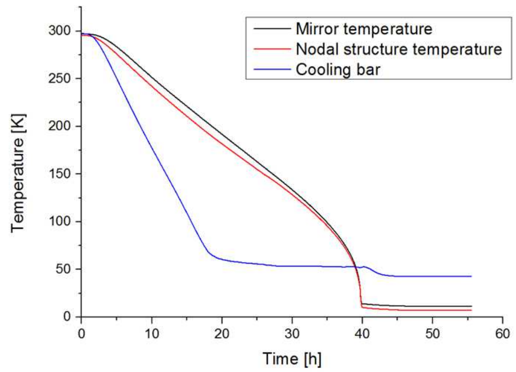

Figure 14: Cooling down of the nodal system and the silicon substrate in the ICRR cryostat.

Before performing the Q measurements at cryogenic temperature, we have to calibrate the substrate temperature with respect to a reference temperature (in this case the temperature of the external aluminum structure of the nodal system) since during the actual measurements it is not possible to connect a thermometer to the substrate since it would greatly reduce the Q. Figure 14 shows a delay of only few kelvins between the two temperatures. This indicates that both systems, substrate and aluminum structure, are mainly driven by the same cooling process, probably the radiation one.

Suspended mass test

A homodyne system was developed to measure the Q of the silicon substrate once suspended in the final configuration. In the meantime it was also used to estimate the oscillations induced on a dummy aluminum substrate[8] by seismic noise (Fig.15). The purpose of this test was to develop an adequate control strategy to reduce seismic noise and allow Q measurements at low teperature. The dummy substrate was hung with appropriately sized steel wires with similar stiffness as 1 mm diameter silicon fibers. A suspended mass of about 2 kg causes high recoil losses. For this reason the tests were housed in the ICRR cryostat which has a very rigid mechanical connection to the floor. Unfortunately, the counterpart of a rigid connection is high seismic noise. Indeed the oscillations induced on the suspended mass were so high that it was impossible to lock the homodine with a mirror moved by a simple piezoelectric but a local control system with optical level, magnets and coils is necessary. So the control strategy will be based on that used in the actual GW interferometers [8] and it wll be implemented in the next summer. As mentioned above, the contribution of each element to the total thermal noise will be assessed before final assembly.

[8]Dimensions and weight similar to those of the silicon substrate.

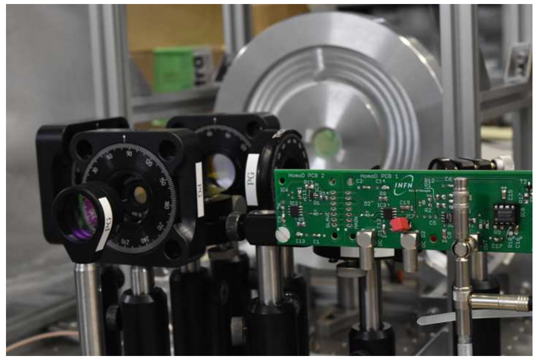

Figure 15: Homodyne system used for Q measurements.

Conclusions

To design and implement a silicon monolithic suspension, it is essential to study and characterize each of its single elements and evaluate the interaction between them in order to optimize the final design of the complete payload. In this perspective we first studied the silicon fibers produced with different methods by measuring some of their mechanical, thermal and chemical characteristics. As regards the grinded-etched fibers, the low quality of their surface was a limit for both mechanical losses and breaking strength (Fig.6). To have better surfaces, tests are ongoing using deeper etching process and thermal treatments by pulsed laser. The silicon-silica fibers were not affected by surface problems (Fig.10) but nevertheless they too showed extra losses due to the friction between the core and the cladding (Fig.9): the removal of the silica cladding through hydrofluoric acid is already partially done (Fig.11) and will be completed in the coming weeks. A common source of extra losses was identified in the clamps used to tighten the fibers (Fig.3), new optimized clamps are already in production. All the fibers were analyzed using an EDX-SEM: no contaminants were found in the pure silicon fibers or in the pure silicon cores (Fig.10) but some bulk imperfections were found in the Czochralski grinded-etched fibers that have further reduced their breaking strength (Fig.5). Due to the thermal conductivity measurements, Float Zone fibers should have a higher quality silicon (Fig.7): their breaking strength will be measured in the next weeks. As for the silicon-silica core, we have no indications on the presence of defects, therefore the first non-destructive tests to be performed will be the measurement of thermal conductivity at low temperatures, the X-ray analysis along the entire silicon core, the evaluation of the loss angle and finally the measurement of the breaking strength.

Measurements of the thermal conductivity of silicon fibers (Fig.7) showed a trend dependent on the production method with higher results for the fibers produced with the float zone method. Instead the silicon-silica fibers showed a trend that was the compromise between the properties of silicon and those of silica. This result suggests the possiblity to develop new strategies to join the fibers with the heads: it will take at least a year to get results on this line of research.

A nodal system was designed, developed, tested and optimized to work at low temperature with substrate of about 20cm in diameter (Fig.12 and 13). Furthermore, the substrate temperature was calibrated with respect to the temperature of the nodal system structure.

Finallly, the homodine for the Q measurement was successfully tested (Fig.15). In the meantime, it was also used to develop a control strategy to reduce the seismic noise on the suspended mass thus to allow Q measurements inside the cryostat. The control strategy thus defined will be based on that used in the current GW interferometers and will be implemented in the coming months.

Acknowledgments

This work was (partially) supported by the Collaborative Inter-University Research Program of the Institute for Cosmic Ray Research (ICRR), the University of Tokyo.

References

[1] http://www.et-gw.eu/index.php/etdsdocument
[2] https://arxiv.org/ftp/arxiv/papers/1907/1907.04833.pdf
[3] The KAGRA Collaboration, Phys. Rev. D **88**, 043007 (2013)
[4] Marc J. Madou, Solid-State Physics, Fluidics, and Analytical Techniques in Micro- and Nanotechnology CRC Press (2011) ISBN 9781420055115
[5] Mohamed Gad-el-Hak, MEMS: Design and Fabrication CRC Press (2005) ISBN 9780849391385
[6] K. E. Petersen, Proceeding of the IEEE **70**, 420-457 (1982)
[7] F. Travasso and Virgo Collaboration, J. Phys.: Conf. Ser. **957**, 012012 (2018)
[8] L. Naticchioni and Virgo Collaboration, J. Phys.: Conf. Ser. **957**, 012002 (2018)
[9] P. R. Saulson, Phys. Rev. D **42**, 2437 (1990)
[10] [J. Czochralski, Z. Phys. Chem. **92**, 219 (1918)
[11] H. C. Theuerer, US Patent 3,060,123 (1962)
[12] H. B. Callen and R. F. Greene, Phys. Rev. **86**, 702 (1952);
[13] H. B. Callen and T. A. Welton, Phys. Rev. **83**, 34 (1951).
[14] Yu. Levin, Physical Review D **57**, 659 (1998)
[15] G. Cagnoli et al., Phys. Lett. A **255**, 230–235 (1999)
[16] G. Cagnoli et al., PRL **85**, 2442 (2000)
[17] S. Reid, G. Cagnoli, D.R.M. Crooks, J. Hough, P. Murray, S. Rowan, Phys. Lett. A **351**, 205-211 (2006)
[18] J. Ballato, T. Hawkins et al., Optics Express **16**, 18677 (2008)
[19] A. C. Peacock, U. J. Gibson and J. Ballato, Advances in Physics: X **1**, 114-127 (2016)
[20] F. Travasso et al., EPL **80**, 50008 (2007)
[21] I. Barducci and G. Pasqualini, Il Nuovo Cimento V **5**, 416-446 (1948)
[22] Kenji Numata et al., Tsubono, Phys. Lett. A **276**, 37 (2000)
[23] Kenji Numata et a.l, Tsubono, Phys. Lett. A **284**,162 (2001)
[24] E. Cesarini et al., Rev. Scient. Instr. **80**,053904 (2009)
[25] A. Dari, F. Travasso, H. Vocca and L. Gammaitoni, Class. Quantum Grav. **27**, 045010 (2010)